

Available online at [www.sciencedirect.com](http://www.sciencedirect.com)**ScienceDirect**

Procedia Engineering 147 (2016) 735 – 740

**Procedia  
Engineering**[www.elsevier.com/locate/procedia](http://www.elsevier.com/locate/procedia)

11th conference of the International Sports Engineering Association, ISEA 2016

## Smart oar blade for hydrodynamic analysis of rowing

Franz Konstantin Fuss\*, Sandra Fundel, Yehuda Weizman, Robert Masterton Smith

*School of Aerospace, Mechanical and Manufacturing Engineering, Sports Technology and Engineering Research Team SportzEdge, RMIT University, Melbourne, VIC 3083, Australia*

### Abstract

A smart oar blade with piezoresistive sensors on either side was developed, calibrated, and tested hydrostatically, hydrodynamically and during rowing. The hydrostatic test down to a water depth of 0.7 m returned the correct and expected pressure values ( $r^2 = 0.9953$ ). In the hydrodynamic test, the peak differential pressure ranged from 100 Pa to 150 Pa, corresponding to a blade velocity and displacement of approximately 0.5 m/s and 0.5 m. In the rowing tests, the peak differential pressure was approximately 800 Pa, corresponding to a blade velocity and displacement of approximately 1.15 m/s and 0.9 m. The large displacement may result from the shape of the boat (gentlemen's skiff) and its load (3 people).

© 2016 The Authors. Published by Elsevier Ltd. This is an open access article under the CC BY-NC-ND license (<http://creativecommons.org/licenses/by-nc-nd/4.0/>).

Peer-review under responsibility of the organizing committee of ISEA 2016

*Keywords:* smart oar blade; pressure sensor; hydrostatic pressure; hydrodynamic pressure, differential pressure, blade velocity, blade displacement, rowing

### 1. Introduction

Forces acting on oar blades can be measured from instrumenting the oar handle, shaft or lock with strain gauges [1]. Commercial products currently available are the PowerLine Boat Instrumentation System (Peach Innovations, Cambridge U.K.), measuring the force at the oar lock, and SmartOar (Boulder CO, USA), measuring the blade force from the bending of the shaft.

To the best of the authors' knowledge, the measurement of the blade force with pressure sensors attached to the surfaces of the blade has never been attempted.

Therefore, the objectives of this study are threefold:

- to instrument a flat oar or paddle blade with pressure sensitive material;
- to measure hydrostatic and hydrodynamic (drag) pressure; and
- to determine the hydrodynamic pressure and its differential when rowing, and calculate the blade's velocity and force from the differential pressure.

### 2. Method

#### 2.1. Development of the smart blade

For instrumenting a wooden plate, a low-cost but highly accurate sensor made of a conductive piezo-resistive polymer (Rmat2a, RMIT material code) was selected. The size of the sensor was 0.16 x 0.16 m large and 0.1 mm thick. Two sensor layers were sandwiched between two aluminium foil electrodes (Fig. 1a). The wooden plate was instrumented on both sides. Each sensor was connected to a 100  $\Omega$  reference resistor in series, and the voltage signal was recorded across the reference resistor with a microcontroller (Teensy3.1, LLC, Sherwood, Oregon, USA) running at a baud rate of 9600 bits per second with a 12 bit analog to digital converter resolution. The microcontroller code was developed with Arduino software (Arduino, Ivrea, Italy).

\* Corresponding author. Tel.: +61 3 9925 6123.  
E-mail address: [franz.fuss@rmit.edu.au](mailto:franz.fuss@rmit.edu.au)

The data were recorded at 10 Hz (hydrostatic/dynamic tests) and 100 Hz (rowing tests) sampling rate frequency. The drop voltage across the reference resistor was used to calculate the conductivity of the sensor material:

$$\sigma = \frac{d}{A} \left( \frac{V_{REF}}{V_{IN} \cdot R_{REF} - V_{REF} \cdot R_{REF}} \right) \quad (1)$$

where  $\sigma$  is the conductivity of the sensor,  $d$  is the thickness of the sensor material (0.2 mm),  $A$  is the area,  $V_{IN}$  is the voltage of the power supply (3.3 V),  $R_{REF}$  is the reference resistance, and  $V_{REF}$  is the measured drop voltage across the reference resistor. The sensor material was calibrated with different number of layers before instrumenting the wooden plate. Two layers of material provided the highest  $r^2$  value of pressure  $p$  against conductivity  $\sigma$  ( $r^2 = 0.9967$ ), when using the power function of

$$p = 97282000 \sigma^{1.184335} \quad (2)$$

The instrumented wooden plate (0.2 x 0.3 x 0.01 m) was connected to an aluminium tube (OD: 0.032 m, wall thickness: 0.003 m, length: 2 m) and made waterproof. Initial hydrodynamic tests indicated that the smart blade did not respond to hydrodynamic pressure but recorded the hydrostatic pressure accurately. Subsequently, an additional wooden plate (0.16 x 0.16 m, 0.003 m thick) was added on top of each outer electrode (Fig. 1b). The final prototype of the smart blade is shown in Fig. 2.

Note that standard oar blades (macon, big blade) are curved in order to generate lift in addition to drag [2]. In this study, however, the smart blade is flat for two reasons:

- 1) as the angles of attack were not measured in this study, the ratio of the individual velocity components responsible for drag and lift were unknown and so too were the changing drag and lift coefficients;
- 2) the pressure sensors had to be placed between two rigid surfaces, the curvature of which, in the case of a curved blade, must be identical; these matching surface curvatures are far more difficult to manufacture than flat plates.

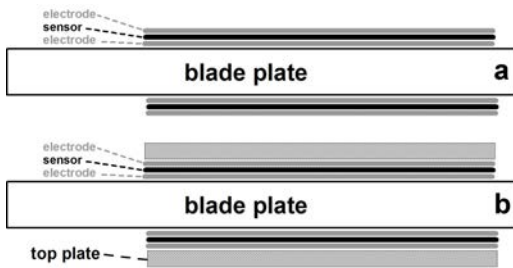


Fig. 1. Sensor arrangement without (a) and with (b) rigid top plates.

Fig. 2. Final prototype with top plates

## 2.2. Hydrostatic and hydrodynamic tests

The oar (Fig. 2) was dipped into a lake such that the centre of the sensor was submerged by 0.2 m. Then the water depth at the sensor was increased incrementally by 0.1 m up to 0.7 m and the process was reversed back to 0.2 m. After each depth increase the blade was kept at this depth for 0.5-2 s. Subsequently, at a water depth of approximately 0.2 m, the blade was moved forward and backward repetitively, for approximately 0.5 m overall displacement.

## 2.3. Rowing tests

The smart blade was tested when rowing on a river (Fig. 3). The rowing boat, a gentlemen's skiff, was loaded with three persons (authors of this paper), one rowing the boat, the second recording the data on a laptop, and the third one photo-documenting the experiment. The stroke rate was approximately 24 strokes per minute (0.4 Hz).

## 2.4. Data processing

The recorded ASCII sensor data (0-4095) were converted to voltage and finally to conductance using Eqn (1). The conductance was converted to pressure using Eqn (2). For the hydrostatic tests,

$$p = D\rho g \quad (3)$$

where  $D$  is the water depth of the centre of the sensor,  $\rho$  is the density of water, and  $g$  is the gravitational acceleration. The results of Eqn (3) were compared to the pressure determined from the sensor data and correlated to each other.

For the hydrodynamic and rowing tests, the differential pressure  $\Delta p$  between the two sensors was calculated. The velocity  $v$  of the moving blade resulted from the drag equation

$$v = \sqrt{\frac{2\Delta p}{C_D \rho}} \tag{4}$$

where  $C_D$  is the drag coefficient. In flat plates, the  $C_D$  is approximately 1.2 [3,4] for  $Re = 150,000-350,000$  (hydrodynamic and rowing tests, respectively). Integration of Eqn (4) with time results in the displacement of movement distance of the blade.



Fig. 3. smart blade used when rowing and recording of data

### 3. Results

#### 3.1. Hydrostatic tests

The results of the hydrostatic tests are shown in Fig. 4. The calculated pressure from the sensor signal (Fig. 4a) matched actual pressure from Eqn (3), with a gradient and  $r^2$  very close to unity (through origin regression fit; Fig. 4b).

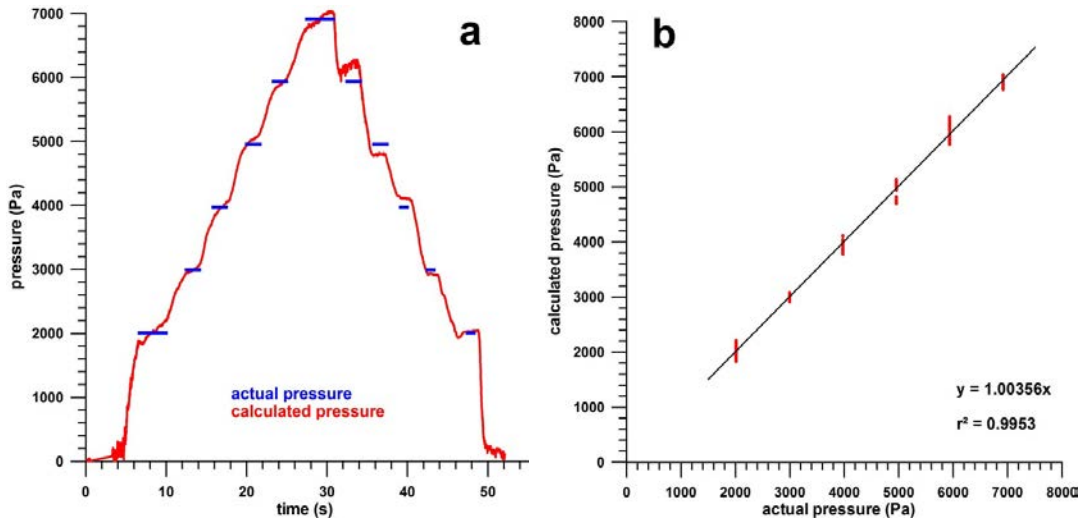


Fig. 4. Hydrostatic tests: (a) actual (blue) and calculated (red) pressure against time; (b) correlation of calculated against actual pressure.

#### 3.2. Hydrodynamic tests

The results of the hydrodynamic tests are shown in Fig. 5. Fig. 5a displays the pressure fluctuations of the two sensors during nine strokes. The expected pattern of increasing and decreasing pressure of repetitive forward/backward motion was clearly

visible in seven strokes on one sensor (black curve), but only in four strokes on the other sensor (red curve). The average of the data of the two sensors during the hydrodynamic tests was approximately 4000 Pa, which corresponded to the average hydrostatic pressure, i.e. the centre of sensor was submerged by 0.4 m on average. In contrast to the hydrodynamic data, the differential pressure exhibited an even fluctuation pattern (Fig. 5b). The velocity pattern was even more consistent as the velocity is a square function of the differential pressure (Fig. 5c). The peak velocity of the blade was approximately 0.5 m/s. The average displacement of the blade was approximately 0.5 m (Fig. 5d).

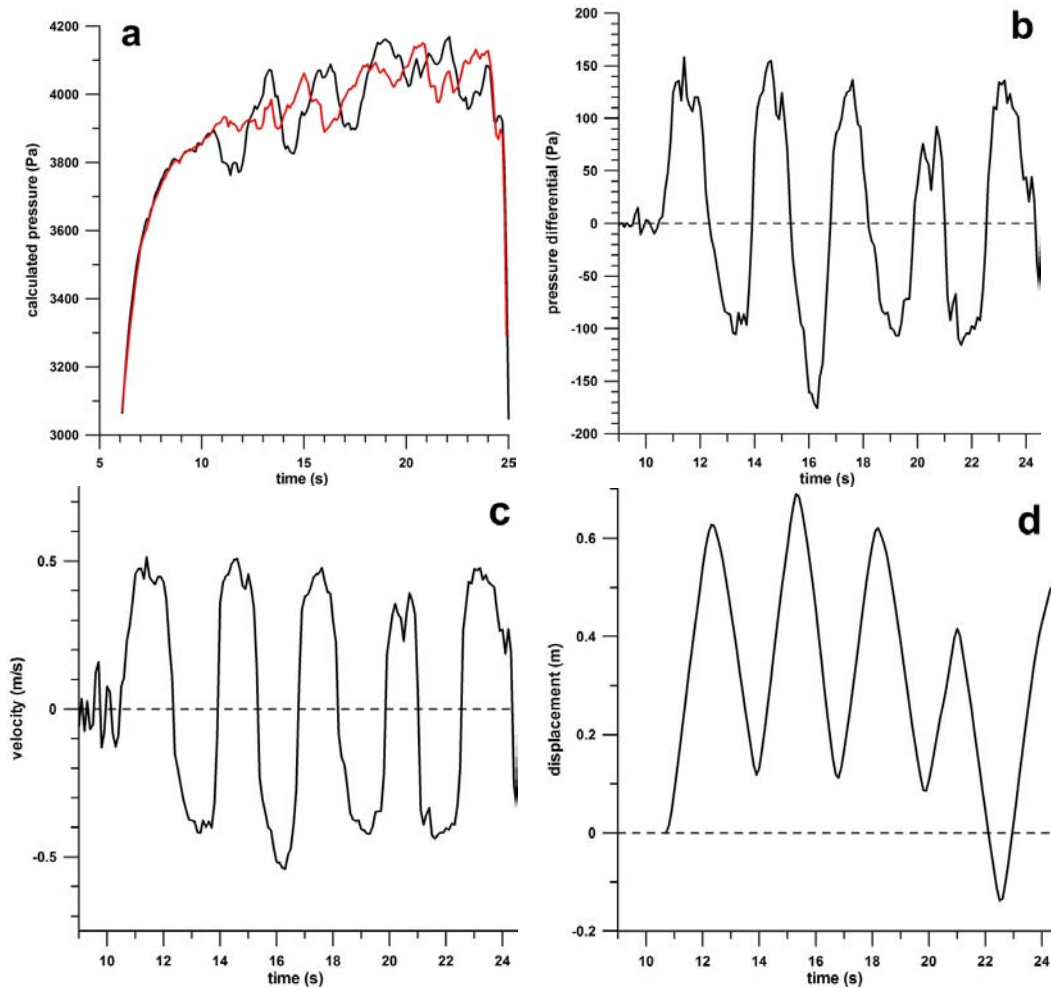


Fig. 5. Hydrodynamic tests: pressure (a) at the sensors (red and black curves denote the two sensors on either side of the plate), differential pressure (b), blade velocity (c) and blade displacement against time.

### 3.3. Rowing tests

The data of seven strokes of the rowing tests are shown in Fig. 6. The average front peak pressure was 1350 Pa (the front sensor corresponds to the front side of the rower); the average rear peak pressure was 750 Pa (Fig. 6a). The average of the peak data of the two sensors during the rowing strokes was approximately 1050 Pa, which corresponded to the average hydrostatic pressure, i.e. the centre of sensor was submerged by 0.0105 m on average. The peak differential pressure fluctuated between 730-825 Pa (Fig. 6b). The peak velocity of the blade was 1.14 m/s on average (Fig. 6c) and the displacement of the blade was 0.9 m on average. The stroke frequency was approximately 0.4 Hz (24 strokes per minute).

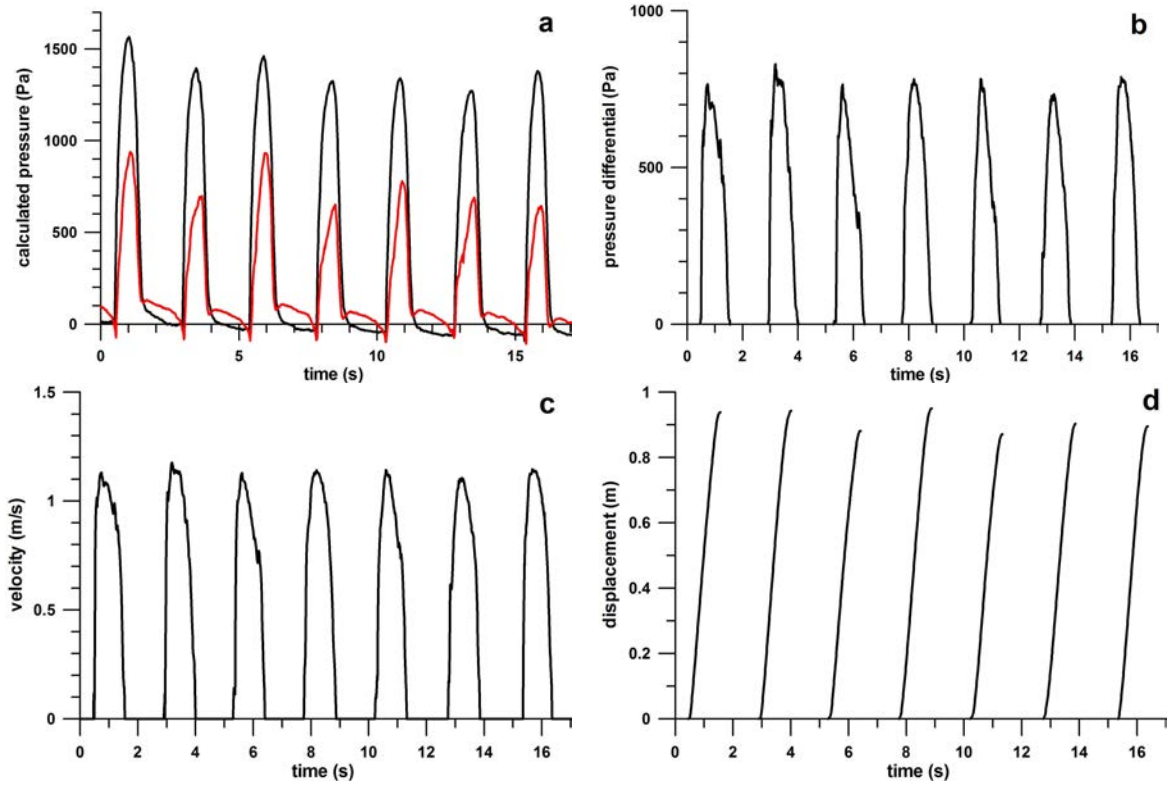


Fig. 6. Rowing tests: pressure (a) at the sensors (black and red curves denote front and rear sensors of the blade; the higher pressure is located on the front side), differential pressure (b), blade velocity (c) and blade displacement against time.

## 4. Discussion

### 4.1. Data processing

As the hydrostatic pressure applied to a blade increases linearly with the immersion depth, the average pressure (e.g. at the centre of the sensor) corresponds to the average water depth. However, the relationship between the pressure and the conductivity of the sensor follows a power law, i.e. a non-linear function, the non-linearity introduces an error such that the average pressure is not exactly at the centre of the sensor. The effective conductivity  $\sigma_{eff}$  of the sensor area over a water depth  $D$  from  $D_1$  to  $D_2$  is calculated from individual conductivities  $\sigma$  (at defined  $D$ )

$$\sigma_{eff} = \frac{1}{\Delta D} \int_{D_1}^{D_2} \sigma \, dD \tag{5}$$

Solving Eqn (2) for  $\sigma$ , and replacing the exponent of the power function by  $b$ , and the multiplier by  $c$

$$\sigma = \sqrt[b]{\frac{p}{c}} = \left(\frac{p}{c}\right)^{\frac{1}{b}} \tag{6}$$

Substituting Eqn (3) into (6) and (6) into Eqn (5), and solving for  $D$ , yields

$$D_{eff}^{\frac{1}{b}} = \frac{1}{\Delta D} \int_{D_1}^{D_2} D^{\frac{1}{b}} \, dD \tag{7}$$

(note that  $\sigma$  is replaced by  $p$ ,  $b$  and  $c$ ; and  $\rho$  by  $D$ ,  $\rho$  and  $g$ ; and that the constants  $c$ ,  $\rho$  and  $g$  are cancelled out). After integration

$$D_{eff} = \left[ \frac{b}{\Delta D(b+1)} \left( D_2^{\frac{1}{b}+1} - D_1^{\frac{1}{b}+1} \right) \right]^b \quad (8)$$

If  $b = 1$ , i.e. a linear function,  $D_{eff}$  equals the average of  $D_1$  and  $D_2$ . If  $b = 1.184335$ , cf. Eqn (2),  $D_1 = 0.015$  m, and  $D_2 = 0.175$  m ( $\Delta D$  equals the height of the sensor, 0.16 m),  $D_{eff}$  is not at 0.095 m, but rather at 0.09305 m, which introduces an error of 1.22%. If  $D_1 = 0.62$  m, and  $D_2 = 0.78$  m (maximal immersion depth of the hydrostatic test), then  $D_{eff}$  is not at 0.7 m, but rather at 0.69976 m, which introduces an error of 0.15%. The greater the water depth, the smaller is the error.

#### 4.2. Hydrodynamic tests

The unsteady hydrodynamic stroke pattern (Fig. 5a) resulted from the fact that it was difficult to keep the immersion depth constant. Although the peak blade force was approximately only  $\pm 10$  N, it had to be applied over a moment arm of 2.25 m (midpoint between the hands holding the shaft) resulting in a moment of 22.5 Nm. The hands of the person conducting the hydrostatic and –dynamic tests, holding the shaft of the blade, were 0.5 m apart, resulting in hand forces of 40 N (upper) and 50 N (lower). The blade also tended to slip sideways such that the shaft had to be stabilized in sideways direction as well.

#### 4.3. Rowing tests

The rowing test exhibited a steady motion pattern (expert rower, multiple gold medalist, senior class) as peak differential pressure (Fig. 6b) and peak velocity (Fig. 6c) were relative consistent. The fluctuations of the calculated pressure (Fig. 6a) were due to slight differences in the blade immersion depth. The net displacement of the blade (opposite to the direction of the moving boat) caused by positive drag differential pressure (Fig. 6 b) was approximately 0.9 m. The blade displacement in propulsive direction stated in the literature is 0.12 m (20 strokes  $\text{min}^{-1}$ ) and 0.17 m (36 strokes  $\text{min}^{-1}$ ) (figure 4 of [5]), and 0.2 m (unknown stroke frequency) (figure 1 of [6]). This displacement corresponds to phase 3 of the blade slip (figure 3 of [2]), when the blade experiences exclusive drag forces. The blade displacement of 0.9 m derived in the present study seems to be excessive. However, it has to be taken into account that the literature data are applicable to single sculls [5] and standard competitive rowing boats (single to eight, light and heavy weight [6]). In our rowing experiment, however, the boat design was different (gentlemen's skiff with wide hull) and moreover, it was loaded with three people. Even if the own stroke frequency (24  $\text{min}^{-1}$ ) matched the one of [5] (20-36  $\text{min}^{-1}$ ), the speed of our boat was far less than that of a single scull. This is also reflected in the peak blade force, which was approximately 44-50 N (differential pressure times the total area of the blade). For single sculls ([1] three different types of blades, four different stroke rates 20-31  $\text{min}^{-1}$ , boat speed 3.5-4.6 m/s or 12.6-16.6 kph), the blade forces reported in the literature were 77-97 N [1], i.e. twice as high as our results. The estimated speed of our boat, however, was less than 6 kph.

Eqn (4) uses constants related to simplified conditions, such as  $C_D$  and the density  $\rho$ . The density, however, changes once air bubbles are introduced through the blade into the water (ventilation; often incorrectly referred to cavitation). The rower, however, took utmost care to prevent any ventilation. Nevertheless, the net movement of the blade should be verified with electrogoniometers at the oarlock and boat speed measurements.

This study was designed as a feasibility test for examining how accurate pressure measurements are, whether the dynamic pressure can be assessed and which other parameters can be calculated from the dynamic pressure. In order to use such a pressure system for competitive rowing, it has to be considered that professional oar blades are curved; this means that a single sensor is not feasible, and that the plastic foil used for waterproofing has to be glued to the top-plates of a sensor matrix sensors. A higher density of sensors distributed over the blade's surfaces would also increase the accuracy of the pressure measurement.

#### References

- [1] Kleshnev V. Points of force application to the oar and efficiency of various blade designs. Bruce ACT: Australian Institute of Sport; 2003.
- [2] Caplan N, Gardner TN. A fluid dynamic investigation of the Big Blade and Macon oar blade designs in rowing propulsion. J Sports Sci 2007; 25(6):643-50.
- [3] Hoerner SF. (1965). Fluid-dynamic drag. Bakersfield CA: Hoerner.
- [4] Crowe CT, Elger DF, Roberson JA. Engineering Fluid Dynamics. 7<sup>th</sup> ed. New York: Wiley; 2001.
- [5] Hofmijster MJ, Landman EHH, Smith RM, Van Soest AJK (2007) Effect of stroke rate on the distribution of net mechanical power in rowing. J Sports Sci 2007; 25(4):403-11.
- [6] Kleshnev V. Propulsive efficiency of rowing. In: Sanders RH, Gibson BJ, editors. Proceedings of the XVII International Symposium on Biomechanics in Sports, Edith Cowan University: Perth, Australia; 1999. p. 224–8.